Chinese Journal of Physics 90 (2024) 266–274

Contents lists available at ScienceDirect

Chinese Journal of Physics

journal homepage: www.sciencedirect.com/journal/chinese-journal-of-physics

Variation of cation-ligands XAl_2Ge_2 (X = Pr, Nd, Gd, Tb) compounds by employing density functional theory

Zeshan Zada [a], Abdul Ahad Khan [b], Ali H. Reshak [c,d,e,*], Dania Ali [f], Muhammad Faizan [g], Qaisar Khan [h], Muhammad Ismail [i], G. Murtaza [a,j], Muhammad M. Ramli [d]

[a] Materials Modeling Lab, Department of Physics, Islamia College University, Peshawar, 25120, Pakistan
[b] School of Engineering and Built Environment, Gold Coast Campus, Griffith University, QLD, 4222, Australia
[c] Physics Department, College of Science, University of Basrah, Basrah, 61004, Iraq
[d] Center of Excellence Geopolymer and Green Technology (CEGeoGTech), University Malaysia Perlis, 01007, Kangar, Perlis, Malaysia
[e] Al-Kunooz University College, Basrah, Iraq
[f] Faculty of Medicine, Charles University, Pilsen, 30100, Czech Republic
[g] Department of Physics, University of Peshawar, Peshawar, 25120, Pakistan
[h] Department of Physical and Biological Sciences, Islamia College Peshawar, Peshawar, 25120, Khyber Pakhtunkhwa, Pakistan
[i] School of Environment and Chemical Engineering, North China Electric Power University, Beijing, 102206, China
[j] Department of Mathematics & Natural sciences, Prince Mohammad Bin Fahd University, P. O. Box 1664, Al Khobar, 31952, Kingdom of Saudi Arabia

ARTICLE INFO

Keywords:
Intermetallic
DFT
Magnetic properties
Ferromagnetism

ABSTRACT

The present report aims to examine detailed Cationic ligands replacement for XAl_2Ge_2 (X = Pr, Nd, Gd, Tb) compounds by employing the density functional theory (DFT) within full-potential linear augmented plane wave (FP LAPW) method. For the structural determination, the generalized gradient (PBE-GGA) approximation has been used to get theoretical reliable and analogous results with the available experimental data. We have further established that the ferromagnetic phase is more stable and suitable for calculation of the magnetic properties. The two approximations namely (PBE-GGA and GGA+U) are used for the investigation of band structures. The band structures along with density of state (DOS) plots approve the metallic character of XAl_2Ge_2. There exists a strong hybridization between (Pr, Nd, Gd, Tb) f and (Al, Ge) s, p states. Also, the examination of magnetic properties confirms a strong ferromagnetism in XAl_2Ge_2 compounds.

1. Introduction

In the last few years, interest in intermetallic compounds has been increasing due to their perplexing properties and various scientific and innovative applications. These intermetallic compounds have a specific electronic structure making them liable for numerous properties at quantum level. Normally, intermetallic phase shows enormous effect in the broad range of applications from computer read, shape memory alloys, dentistry and jewelry [1,2] and mostly utilized for innovative outcomes as “colossal magneto-resistive (C-M-R)” or else “giant magneto-resistive (G-M-R)” materials where magneto-resistance inside metallic thin films is capable of altering and adjusting resistivity due to the presence of external magnetic field [3,4]. Despite the fact that the significant

* Corresponding author.
E-mail address: maalidph@yahoo.co.uk (A.H. Reshak).

https://doi.org/10.1016/j.cjph.2023.12.002
Received 6 September 2023; Received in revised form 11 November 2023; Accepted 3 December 2023
Available online 4 December 2023

application of GMR can be fundamentally utilized as spin filters, spin valves, and magnetic field sensors [5] as well, the primary uses of GMR is important for magnetic sensors, which are practically used to read-heads in the hard disk drives, biosensors, micro-electro-mechanical systems (M-E-M-S)[6], and so on.

In general, intermetallic phases having the formula $AM_2\times_2$ (A = rare-earth metals/alkaline-earth metals, M = d-block metals; X = Group 13–15 elements) incorporate two ubiquitous structure types, with space groups namely $ThCr_2Si_2$ (14/mmm) [7] and $CaAl_2Si_2$ ($P\overline{3}m1$) [2], correspondingly. Researchers on the other side have used different crystal structure types to show that the prerequisite for the arrangement of pristine ($CaAl_2Si_2$) structure type is recognized as the whole numeral of (valence electrons) primarily present in per formula unit should be equivalent to or under 16 [8–10]. The formerly known Pnictide AM_2Y_2 (A: (electro-positive) Element; M: metals; Y: P to Bi) follows with no exception into this arrangement; which at first in repudiated affiliations with $L_nLi_2Y_2$ (L_n: Pr, Ce, Tb, Nd; Y: P to Bi) [11–13] but later on effectively changed into only ($L_nLi_3Y_2$) correct composition [14]. Furthermore, the characterization of well-known silicides ($L_nAl_2Si_2$) and Layered ligand-germanides was done by using the chemical formula of ($L_nAl_2Ge_2$) persevere [15–18], which basically crystallize in the ($CaAl_2Si_2$) pristine crystal structure, as revealed for example $[Ln^{3+}(Al^{3+})_2(Si^{4-})_2]$ with absent valance composition.

Taking into account the structural information of $GdAl_2Si_2$ [18] shows a comparable distribution of cation-ligands as per the given formula which is similar and should be appropriate for other cases like Germanide, moreover it has a specific outward perspective to benefit from this linking similarity to consider their electronic character more powerful. To begin with the silicides (trivalent rare-earth-metals) side, only a crystal-structure determination of $GdAl_2Si_2$ is so far, whereas the lattice constants of other compounds $CeAl_2Si_2$ [19] and YAl_2Si_2 [20] were studied. In addition to this no ambiguity existed in past works but comparable connections with Ln = Gd-Lu, Pr is already set up with no other components of crystallo-graphic data are portrayed [15,16].

The synthesis of the compounds $L_nAl_2Si_2$ (L_n: Y, trivalent rare-earth-metal) was done by rising the temperature range from 800° up to 1000 °C. They are further crystallized in the pristine structure type namely ($CaAl_2Si_2$) with space group (P 3′ m1; $Z = 1$) and it fits to reported isotypic [21]. For the band structure investigation of both ($CaAl_2Si_2$ and YAl_2Si_2), LMTO code was designed, the later YAl_2Si_2 affirms non-electrovalent makeup concerning to the given formula, and the same compound is also examined in that class by means of electrical conductivity along with the predominantly bonding mechanism side [21]. Due to the material characterization technique, it is clear that motley crystal $GdAl_{2-x}Mn_xSi_2$ shifts from $GdAl_2Si_2$ ($CaAl_2Si_2$) to $GdMn_2Si_2$ ($ThCr_2Si_2$) structure phase by substituting a value of about ($x \approx 0.3$) for Mn. Moreover, the crystallization was done for $EuAl_2Ge_2$, $EuAl_2Si_2$ and $YbAl_2Ge_2$ compounds for the first time in same structural phase by methods of heating from 1070 to 1270 K. Among all the three compounds beyond 50 K the ($EuAl_2Ge_2$ and $EuAl_2Si_2$) examined paramagnetic character. Interestingly, both compounds exhibit antiferromagnetic ordering at specific temperature for $EuAl_2Ge_2$ at T_N = 27.5 K and $EuAl_2Si_2$ at T_N = 35.5 K respectively [22].

The $YbAl_2Si_2$ compound conventional response has distinguished between 100 and 300 K temperature ranges. The linear investigation of inverse susceptibility gives us a specific value of temperature as well as a minor magnetic moment estimation of (Yb) about $2.57\mu_B$ along with extraordinarily inspected negative paramagnetic Curie temperature (T_c) at about −382 K. The degree level of (divalent) ytterbium has developed sharply under temperature 100 K [22]. Besides the non-magnetic $4f^{14}$ reasonable ground states were inspected in Yb basal compounds, whereas close to the Fermi level the high-sharp 4f exhibits the ability to create mediate valency inside $YbAl_2Si_2$. Also, the vanishing band gap is the only fact behind their stability while the existing atoms in $M_2\times_2$ slabs prove a slight electronegativity difference.

By considering this position, the excessive electrons are not responsible for the distortion of the crystal structure, though it happens when the energy bandgap is available. Thus, it is clear that the response like metallic is not because of the presence of the excessive electron, but mostly from the material metallic character itself [21]. Separately, each compound AAl_2Ge_2 and $CaAl_2Si_2$ crystal-structure type is probable to show metallic nature; however the valence shell electron is based on metal A.

The (SEM) and (XRD) are the two well-known techniques so far used for the material characterization of ternary ($DyAl_2Si_2$) and binary ($DySi_2$) silicides with the strong arrangement of both (Al and Si) elements, which further remain unchanged by hardening the phase mixture [23]. Both aluminum based silicides and germanides $AAl_2\times_2$ where A belong to (alkaline or else rare-earth metal) while X belongs to (Ge or Si) [24,25] were crystallized in the known [La_2O_3] type trigonal structure [26], moreover the ordered double-puckered hexagonal layers of Ge (Si) and Al atoms are chemically prearranged along with the presence of intercalated A (cations) atoms. The stability among these significant compounds was surprising because of their slight electro-negativity difference between the double layer atoms. Furthermore, the electron–phonon interaction along with electronic structure have been investigated for (YAl_2Si_2) compound [27].

So far researchers have attempted to examine experimentally some of the physical properties of XAl_2Ge_2 compounds. But till now, the absence of theoretical investigation primarily on structural, electronic and magnetic properties has been absent in the literature chiefly by using DFT. Thus, our concentration in the present research study is generally focused on the improvement of energy band gap to overcome the lack of theoretical data about XAl_2Ge_2 compounds by means of FP-LAPW method.

2. Computational calculations detail

The lanthanide based XAl_2Ge_2 compounds are properly classified as intermetallic phases with trigonal structure geometry of space group (#.164) [29]. For the complete the physical parameters of XAl_2Ge_2 compounds, the density functional theory (DFT) were accomplished [31,32] which is further based on full-potential linear augmented plane wave (FP-LAPW) scheme as implemented in WIEN2K code [33]. The structural relaxation together with optimization have been done by utilizing the generalized-gradient-approximation (GGA-PBE) of Perdew Burke Ernzerhoff [34] and GGA +U [35,36] for treating exchange plus

correlation potential as well. Moreover, the value of (R_{MT}* K_{MAX}) is selected as 7.0 to control the *K* vector larger magnitude in plane wave. A 1000 K points mesh [37,38] in the (BZ) Brillouin zone together with appropriate muffin-tin (RMT) radii like (2.5, 2.16, 2.39) (a.u.) for $PrAl_2Ge_2$, (2.5, 2.09, 2.31) (a.u.) for $NdAl_2Ge_2$, (2.5, 2.17, 2.4) (a.u.) for $GdAl_2Ge_2$ and (2.5, 2.0, 2.23) (a.u.) for $TbAl_2Ge_2$, respectively are selected for these lanthanide-based compounds in suitable ferromagnetic phase. In order to achieve energy eigenvalue convergence, the wave functions in the interstitial region are expanded using plane waves with a cutoff of 7.0. The charge density was Fourier expanded up to Gmax (Gmax = 12 atom unit $(au)^{-1}$). Self-consistency is obtained using 1000 K points

3. Result and discussions

3.1. Structural properties

The XAl_2Ge_2 (X = Pr, Nd, Gd, Tb) compounds has computed in hexagonal-structure geometry [Fig. 1**(a)**] [39], related to the flawless known $CaAl_2Si_2$-structure. The bilayer Al in the structure occurs as a corrugated (puckered) Al honeycomb; however, all these compounds crystallize in the trigonal crystal structure ($CaAl_2Si_2$) having space group $P\bar{3}m1$ with (#164). The broad interpretation of ($ThCr_2Si_2$) structure is still inspiring one among researcher by virtue of numerous compounds so far own this symmetry type and also outline supreme properties concerning $CaAl_2Si_2$ type. While the compounds which are crystallize in $CaAl_2Si_2$ structure symmetry found less in numbers; in view of distinct and accessible features for future electronic flexibility between these two novel types [3,4]. $CaAl_2Si_2$ type is resolved simply by considering the (Al) element at B-site which particularly has (d^{10}, d^5 or d^0) electronic configurations [30]. So, the $CaAl_2Si_2$ type is more sufficient and favorable for $d^{10}$and d^0 configurations as compare to $ThCr_2Si_2$ type.

The XAl_2Ge_2 (X = Pr, Nd, Gd, Tb) compounds show the trigonal crystal geometry as mentioned earlier. The calculated optimized structural parameters and plots of optimization are portrayed in Table 1 and Fig. 2. Moreover, the studied lanthanide material stabilizes in the FM phase. The energy calculations along with computed plots of optimized volume for the four compounds show the favorable nature of the FM configuration.

By volume optimization process the theoretical structural parameters of XAl_2Ge_2 (X = Pr, Nd, Gd, Tb) compounds are achieved by using (PBE-GGA) which consist of lattice parameters (ɑ, c (Å)), bulk modulus, B(GPa) as well as pressure derivative (Bp). To investigate the entire stable energy (E_0) we have utilized the "Birch Murn-aghan's equation of state". The planned optimization plots give appropriate lowest energy of the primitive unit cell [1].

Our reported structure variables are in good agreement with the experimental mentioned values [28,29,30] as noted in Table 1. A clear decrease in the compound lattice constants (*a* (Å) and c (Å)) and volume (V_0) are observed while calculating through both (PM and FM) phases by replacing the cation-ligands from Pr to Tb. The main reasons behind this fall are the decrease in atomic sizes and further increase in electronegativity difference by changing the cations all the way from left to right in the same period. Moreover, the B(GPa) which define compressibility of materials, the calculated values of the investigated compounds for this property show mix peculiar increasing and decreasing trend from Pr to Tb as shown in Table 1.

3.2. Electronic properties

3.2.1. Band structure and density of states

The electronic band structure of XAl_2Ge_2(X = Pr, Nd, Gd, Tb) compounds with spin up and down configurations are shown in (Figs. 3 and 4) by using (GGA-PBE and GGA+U) schemes. The significant information like bonding nature amongst atoms and electromagnetic properties of the material are determined by calculating the band structure. For simplicity, the Fermi-level is taken at zero eV. While the investigated compounds energy band structures are designed alongside the high symmetry (Γ-M-K-Γ-A) points of the

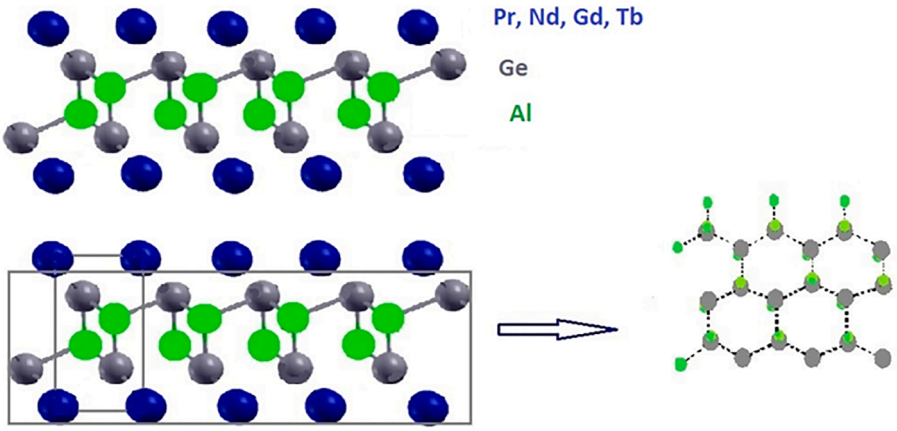

Fig. 1. Crystal formation of XAl_2Ge_2 (X = Pr, Nd, Gd, Tb). Blue spheres: *X*; gray spheres: Ge; green spheres Al. The tetrahedral coordination of (Al atoms) along with Al_2Ge_2 poly-anion is underlined.

Table 1
Calculated values of lattice parameters, (*a, c* (Å)), V_0, B (GPa), Bp and E_0 (Ry) for XAl_2Ge_2(X = Pr, Nd, Gd, Tb) compounds in both (PM and FM) Phases along with previous published works.

Compounds	Lattice a	Constant C	V_0	B(GPa)	BP	E_0 FM	E_0 PM
$PrAl_2Ge_2$**(FM)**	4.2	6.77	747.6391	65.0230	5.0000	−27,853.40	−27,853.34
Exp[a]							
$NdAl_2Ge_2$ **(FM)**	4.261	6.811	736.1338	85.2557	2.5005	−28,627.96	−28,627.82
Exp[b]	4.269	6.832	107.83				
$GdAl_2Ge_2$ **(FM)**	4.251	6.714	725.0322	67.2295	5.0000	−31,928.94	−31,928.39
Exp[c]	4.253	6.716	105.20				
$TbAl_2Ge_2$ **(FM)**	4.231	6.613	656.8720	544.897	5.0000	−32,806.06	−32,805.64
Exp[b]	4.238	6.661	103.61				

[a] Ref. [28].
[b] Ref. [29].
[c] Ref. [30].

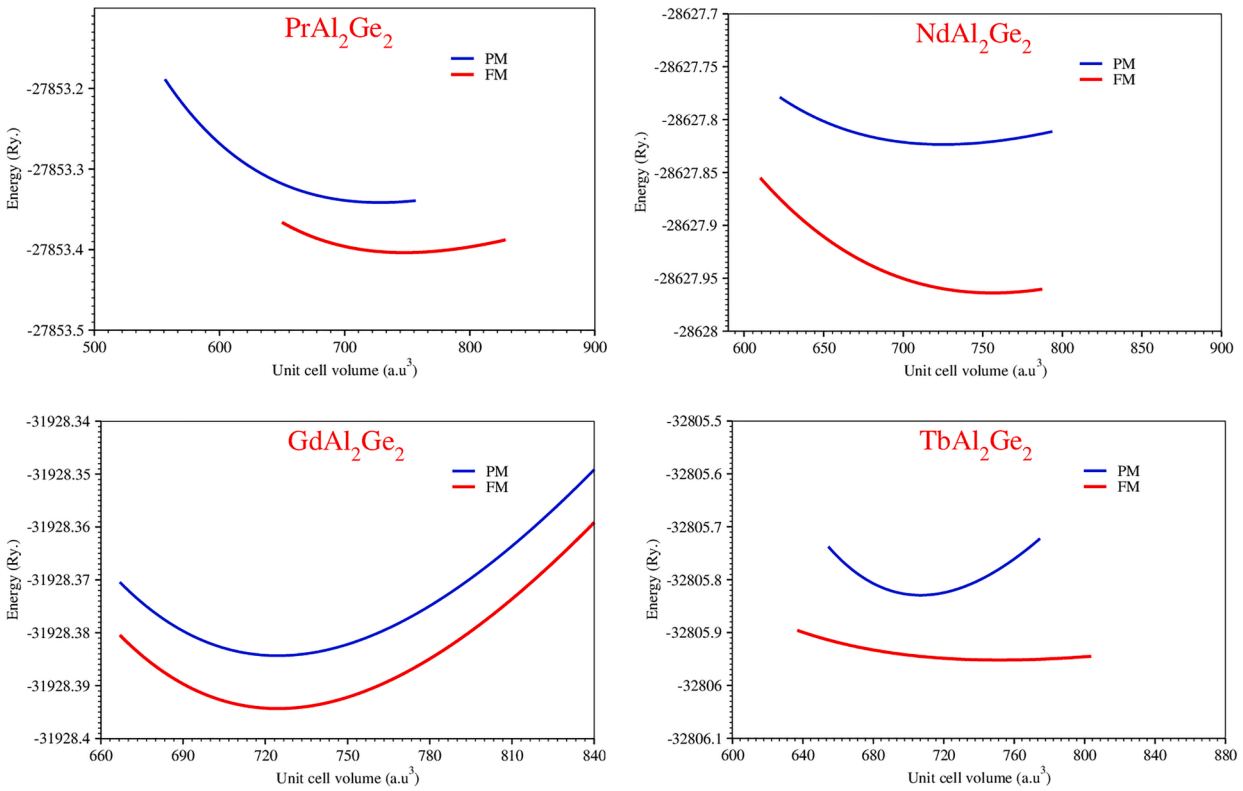

Fig. 2. Optimized plots of XAl_2Ge_2 (X = Pr, Nd, Gd, Tb) compounds.

Brillouin zone (BZ). The compounds valence band maxima through various spin up while some down spin states show leading principal dispersion along basal-plane Γ−K direction, and mostly along the c-axis, the Γ−A line, while conduction band minima show principal dispersion along the whole basal plane in various spin states whereas mostly arise along with high symmetry M and Γ directions through both approximations. This describes that the conductivity of XAl_2Ge_2 is almost in all directions are likely to be strong.

Moreover, the lanthanides (Pr, Nd, Gd, Tb) f character mainly contributed in the minima of conduction band, whereas the Al/Ge elements p character dominantly contributing in the maxima of valence band, apart from this the wide feature is extremely resembling for the XAl_2Ge_2 band structures in spin-up/down configurations.

Though, there are two differences in details first the disappearance of Gd-d orbital in $GdAl_2Ge_2$, second the overlap among the (Al, Ge) s, p and the Gd f orbitals are turning into active. So, the overlapping mechanism between the (valence and conduction) bands are dominant enough in spin-up/down types in $GdAl_2Ge_2$ than the remaining understudy compounds as plotted in (Fig. 5). Furthermore, one has noticed that the plotted bands have (larger and more extensive) dispersion along the M and Γ high symmetry directions, reflecting effective inter-layer coupling in XAl_2Ge_2(X = Pr, Nd, Gd, Tb). Additional significant characteristics in the band structures of XAl_2Ge_2 compounds are the crossing or intersection mechanisms of (valence and conduction) bands together with the Fermi level

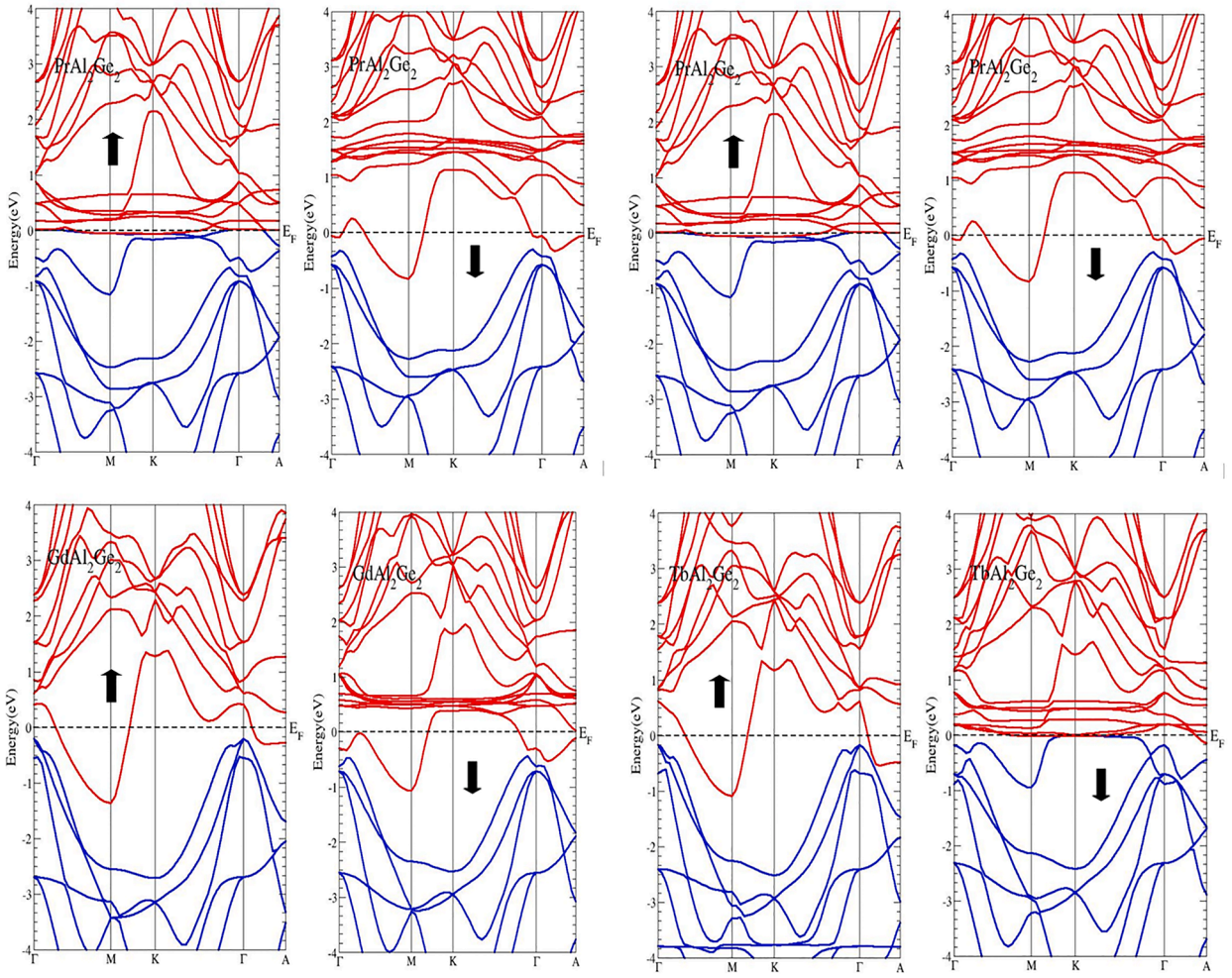

Fig. 3. Band structures of XAl_2Ge_2 compounds in ferromagnetic phase while computing GGA-PBE in spin-up/down configurations.

location in spin-up/down configurations.

The valence band touches both the Fermi level and conduction bands in spin-up state of $PrAl_2Ge_2$ at almost all the high-symmetry points, while in spin-down state it stays below the Fermi level but when it comes to conduction bands it clearly crosses the Fermi level at the high symmetry points (M and Γ), followed by the compound $NdAl_2Ge_2$ with the similar trend through both (GGA and GGA+U) approximations. Moreover, the valence band in $GdAl_2Ge_2$ stays below the Fermi level whereas conduction band cross it deeply at (M and Γ) points in spin-up/down configurations, lastly the compound $TbAl_2Ge_2$ follow the similar trend through spin-up state whereas shows peculiar behavior by touching the Fermi-level and few conduction bands between the high symmetry points (M and Γ) as depicted in (Figs. 3 and 4) for GGA and GGA+U approximations. Thus, the XAl_2Ge_2(X = Pr, Nd, Gd, Tb) compounds display no energy gap at the Fermi-level which further confirm pure conductivity measurements among them.

In XAl_2Ge_2, just a single conduction band mostly crossing the Fermi energy (FE) level at (M and Γ) the high symmetry points appear in majority band structures of spin-up/down configurations. The valence bands are totally filled and has no further need to hold holes for the XAl_2Ge_2 compounds. Finally, the band structure (BS) of XAl_2Ge_2 illustrate metallic behavior because of the overlapping and intersection mechanisms of conduction band minimum together with valance band maximum across the Fermi-level with absent energy gap in spin-up/down configurations.

The benefit of calculating density of state (DOS) function is to explore how much (s/p/d/f) each state share its contribution to both valence and conduction bands. The examinations of DOS verses energy are plotted in the range between (−5 and 5 eV) for XAl_2Ge_2(X = Pr, Nd, Gd, Tb) compounds in Ferromagnetic phase in spin-up/down configurations while utilizing GGA+U approximation as appeared in (Fig. 5). The support of electronic states together with mechanisms among ions are definitely perceived by total and partial (TDOS/PDOS) density of states.

Though, the understudy XAl_2Ge_2 compounds depict full metallic behavior on the grounds that their total and partial (s, p, d, f) density of states curves dominantly crossing the Fermi-level in spin-up/down configurations. Which can further be clarify from the total DOS where the effective improvement at (EF) arises from (Pr, Nd, Gd, Tb) f states. Moreover, there is a solid hybridization of X-f

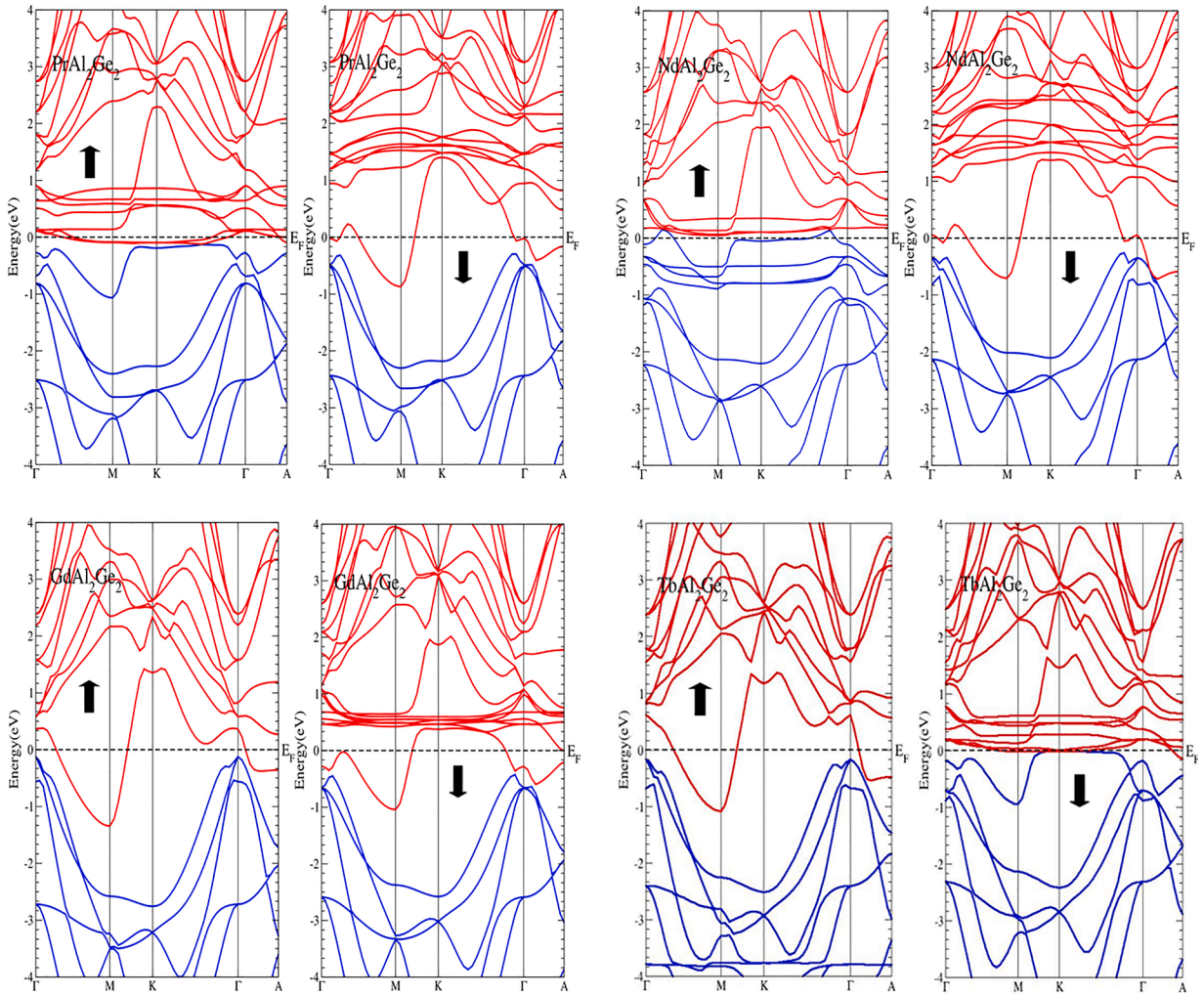

Fig. 4. Band structures of XAl_2Ge_2 compounds in ferromagnetic phase while computing GGA+U in spin-up/down configurations.

states with both (Al and Ge) s, p states lie between the regions of valence/conduction band in spin-up/down configurations. These states are the significant reason for the materials to hold metallic properties. The predominant contribution in $PrAl_2Ge_2$ compound is due to the lanthanide element Pr-f state which arise sharply further a straight line of Pr-d state spread over the entire energy range. While remaining three compounds ($NdAl_2Ge_2$, $GdAl_2Ge_2$ and $TbAl_2Ge_2$) follow the same trend with little changes in detail like the same straight line due to Gd-d state disappeared clearly seen in $GdAl_2Ge_2$ compound by using spin-up/down configurations.

In addition to this the Pr/Nd/Gd/Tb f states display strange behavior on the Fermi point in spin-up orientation and away from the Fermi in the conduction band high energy region at around 1.8 eV with the spin-down orientation of both $PrAl_2Ge_2$ and $NdAl_2Ge_2$ compounds. Apart from this a sharp spike of Gd-f state while peak with a shoulder of Tb-f state appears in the up-spin state aside from the Fermi in the lower valence band region at around −4.7 eV and further remain lies near to the Fermi in both $GdAl_2Ge_2$ and $TbAl_2Ge_2$ compounds with spin-down states. At last, the participation of Al and Ge elements (s, p) states are very comparable over the whole energy range in all the four examined compounds in the valence together with conduction bands area of spin-up/down configurations.

Generally, the DOS of revealed XAl_2Ge_2 compounds illustrate (metallic behavior) in spin-up/down configurations across the Fermi Energy E_f.

3.3. Magnetic properties

In order to achieve more descriptive information about the material magnetic properties along with broad understanding, we have assessed the magnetic measurements in different manners like the $\mathbf{m}^{\mathbf{c}}$ (total each cell magnetic moment) of XAl_2Ge_2(X = Pr, Nd, Gd, Tb) compounds together with their interstitial and individual atomic (X, Al and Ge) magnetic moments by utilizing (PBE-GGA and GGA+U) approximations are indicated in Table 2. All the magnetic moments with non-negative values show that the magnetic ground states of XAl_2Ge_2 compounds are ferromagnetic. The computation through GGA+U gives higher values in contrast with PBE-GGA for

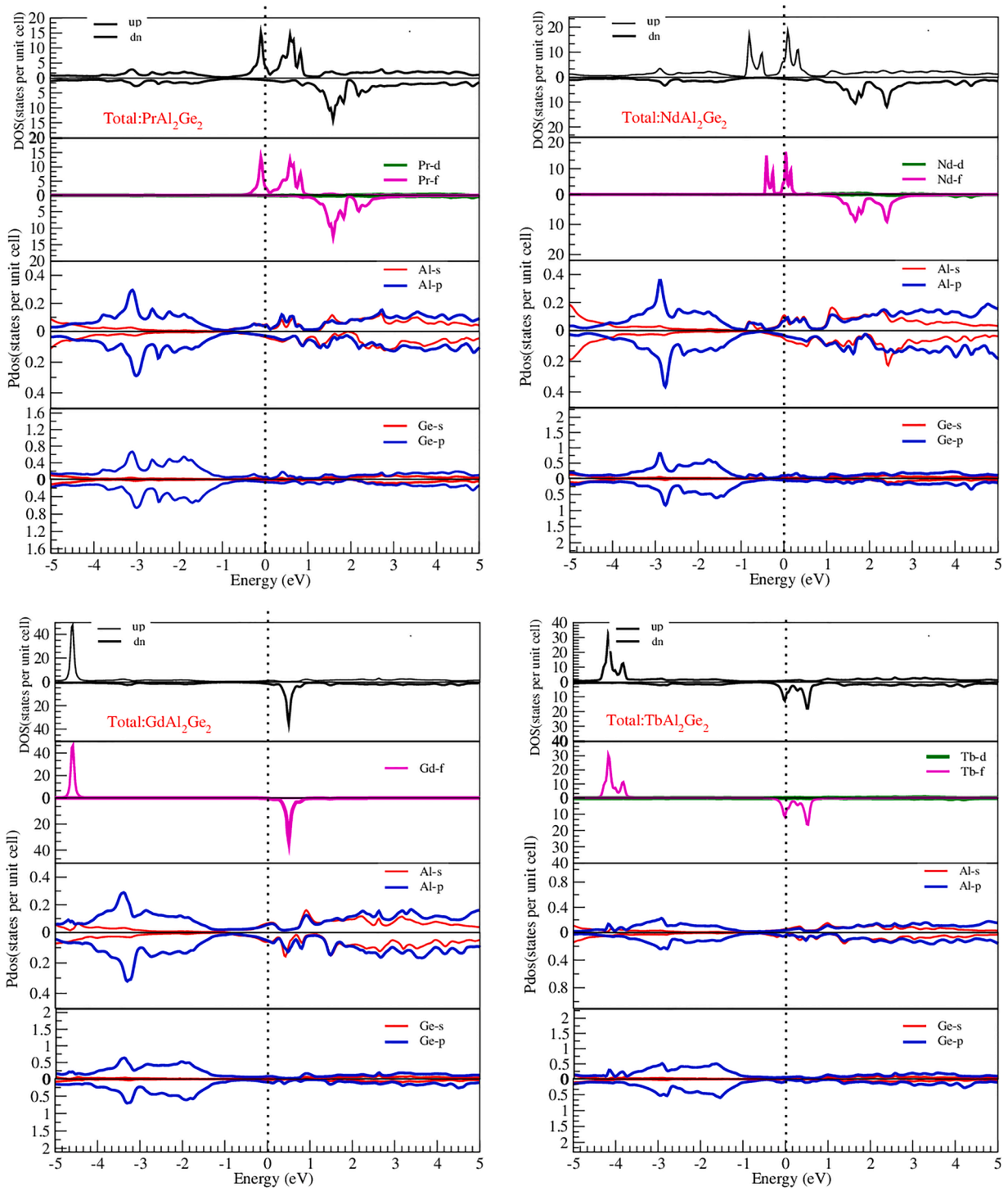

Fig. 5. Plotted DOS of XAl_2Ge_2 compounds in ferromagnetic phase using GGA+U in spin-up/down configurations.

the investigated compounds except $PrAl_2Ge_2$, because (GGA+U) treats localized f/d-shell electrons of (Pr, Nd, Gd, Tb) lanthanide atoms and slightly (increase or decrease) its overall magnetic moment in correlation with other approximations. The magnetic moments of the total cells are primarily composed of the (X = Pr, Nd, Gd, Tb) atoms together with minor contributions in detail of atom at interstitial sites as well as Al/Ge atoms. The X atoms in XAl_2Ge_2 compounds have high values of magnetic moments from the remaining attached atoms. By considering magnetic moment investigation, we have observed that the magnetic moment of the lanthanide (X = Pr, Nd, Gd, Tb) atoms are higher enough as compared to Al/Ge atoms which is primarily because of the f states of the (Pr, Nd, Gd, Tb)

Table 2
Magnetic moments of the interstitial region (m^{inte}), single atoms ($M^{Pr/Nd/Gd/Tb}$) and overall cell for XAl_2Ge_2(X = Pr, Nd, Gd, Tb) compounds computing both schemes (Bohr magnetrons μ_B).

Compounds	m^{inte}	$M^{Pr/Nd/Gd/Tb}$	m^{Al}	M^{Ge}	m^{cell}
$PrAl_2Ge_2$ (PBE-GGA)	0.62155 0.34961	2.24181	0.03758 0.00494	0.02568	2.98990
GGA+U	———	2.14188	———	−0.00544	2.49050
Exp.	———	———	−0.00632[d]	———	———
Other calc.		———		0.00298 [d]	———
$NdAl_2Ge_2$(PBE-GGA)	0.24860 0.32153	3.32957 3.30272	0.00420	−0.01883	3.54891
GGA+U	———	———	0.00514	−0.00918	3.61618
Exp.	———	———	———	———	———
Other calc.			———	———	———
$GdAl_2Ge_2$ (PBE-GGA)	0.17335 0.20145	6.92442	−0.00773	−0.02090	7.04052
GGA+U	———	6.92517	−0.00832	−0.01395	7.08209
Exp.	———	———	———	———	———
Other calc.		———	———	———	———
$TbAl_2Ge_2$ (PBE-GGA)	−0.03397 0.16356	5.68817	−0.02085	−0.01340	5.58569
GGA+U	———	5.74105	−0.00692	−0.01346	5.86385
Exp.	———	———	———	———	———
Other calc.		———	———	———	———

[d] Ref. [40].

atoms emerging predominantly over the whole energy-range in spin-up/down orientations, as depicted in the compound DOS plots (Fig. 5). The major source of magnetization comes from unoccupied X-f orbitals, additionally the X-f states are particularly demonstrating the incomplete or partially filled sub-f states, which clearly valid for ferromagnetism in the investigated compounds. Apart from this, magnetic moment with negative values expresses the true explanation of Al/Ge atoms in the unit cell at all sites offering the rise in anti-parallel participation to the overall ferromagnetic direction because of an employment of other constituent's atoms. Thus, both the aluminum and germanium sites further polarized (anti-parallel magnetic moment) with a negative number and will in general be bring down the materials overall ferromagnetic nature. Also, the determined values through both approximations of the magnetic moment at interstitial site together with total cell for XAl_2Ge_2 compounds supporting while (Al/Ge) opposing the net magnetic moment with the negative decimal numbers. The opposite sign turns out among the magnetic moments of (Inst, X, Al, Ge and total cell) reveals that electrons in their valence band associate in anti-ferromagnetic aspect. The non-integer positive magnetic moments declare that all these four lanthanide-based compounds have solid ferromagnetic metallic-behavior. The contrast inside the two computed values is due to the certainty of (GGA+U over GGA) as noted in Table 2 inside the extremely correlated framework.

4. Conclusions

We have examined the structural, electronic and magnetic properties for XAl_2Ge_2 (X = Pr, Nd, Gd, Tb) basal compounds by employing Full-potential linear augmented plane wave (FP-LAPW) method within density functional theory (DFT). Our theoretical structural parameters of compounds are reliable and analogous with experimental available data. We have further established that FM is more stable than PM phase and also suitable for the calculation of compounds magnetic properties. The two approximations namely (PBE-GGA and GGA+U) are used for the investigation of band structures. The spin-polarized configurations were continuously analyzed by GGA+U scheme by utilizing $U_{eff} = 7$ eV. The calculated band structures along with density of state (DOS) plots approve metallic character of XAl_2Ge_2 by solid hybridization present among (Pr, Nd, Gd, Tb) f and (Al, Ge) s, p states. Also, the examination of high positive magnetic moments confirms strong ferromagnetism in the said compounds.

Declaration of Competing Interest

The authors declare that they have no known competing financial interests or personal relationships that could have appeared to influence the work reported in this paper.

References

[1] K. Masumoto, W.A. McGahan, Electromagnetic applications of intermetallic compounds, MRS Bull. 21 (5) (1996) 44–49, https://doi.org/10.1557/S0883769400035508.
[2] Z. Zada, H. Ullah, R. Zada, A.A. Khan, A. Mahmood, S.M. Ramay, Electronic band profiles, magnetic stability, antiferromagnetic spins ordering and thermodynamics properties of novel antiferromagnet $CaCr_2Sb_2$, Eur. Phys. J. Plus 136 (4) (2021) 1–12, https://doi.org/10.1140/epjp/s13360-021-01356-5.
[3] Z. Zada, A. Laref, G. Murtaza, A. Zeb, A. Yar, First-principles calculations of electronic and magnetic properties of XMn_2Y_2 (X= Ca, Sr; Y= Sb, Bi) compounds, Int. J. Mod. Phys. B 33 (18) (2019) 1950199, https://doi.org/10.1142/S0217979219501996.
[4] Z. Zada, H. Ullah, R. Zada, S. Zada, A. Laref, S. Azam, M. Irfan, Structure stability, half metallic ferromagnetism, magneto-electronic and thermoelectric properties of new zintl XCr_2Bi_2 (X= Ca, Sr) compounds for spintronic and renewable energy applications, Physica B: Condens. Matter (2021) 412866, https://doi.org/10.1016/j.physb.2021.412866.
[5] Z. Zada, A.A. Khan, A.H. Reshak, M. Ismail, S. Zada, G. Murtaza, J. Bila, Cationic variation for LnAl2Si2 (Ln= Y, Sm, Tb, Dy, Yb) compounds by density functional theory, J. Mol. Struct. (2021), https://doi.org/10.1016/j.molstruc.2021.132136, 132136 H.

[6] Z. Zada, R. Zada, A.A. Khan, M. Saqib, M.F.U. Rehman, M. Ismail, M. Faizan, Investigation of electronic structure, magnetic stability, spin coupling, and thermodynamic properties of novel antiferromagnets XMn_2Y_2 (X= Ca, Sr; Y= P, As), J. Mol. Struct. 1268 (2022) 133698, https://doi.org/10.1016/j.molstruc.2022.133698.

[7] R. Bibi, Z. Zada, A.A. Khan, S. Azam, M. Irfan, B.U. Haq, S.A. Khan, First-principles calculations of structural, electronic, magnetic, thermoelectric, and thermodynamic properties of BaMn2P2 in the anti and ferromagnetic phase, J. Solid State Chem. 302 (2021) 122388, https://doi.org/10.1016/j.jssc.2021.122388.

[8] P. Klüfers, A. Mewis, AB2×2-verbindungen im CaAl2Si2-typ, III zur struktur der verbindungen CaZn2P2, CaCd2P2, CaZn2As2 und CaCd2As2/AB2×2 compounds with the CaAl2Si2 structure, III the crystal structure of CaZn2P2, CaCd2P2, CaZn2As2, and CaCd2As2, Z. Naturforsch. B 32 (1977) 753–756, https://doi.org/10.1515/znb-1977-0706.

[9] P. Klüfers, A. Mewis, AB_2X_2-verbindungen mit CaAl2Si2-struktur, Z. Kristallogr.-Cryst. Mater. 169 (1–4) (1984) 135–148, https://doi.org/10.1524/zkri.1984.169.14.135.

[10] A. Artmann, A. Mewis, M. Roepke, G. Michels, AM2×2-verbindungen mit CaAl2Si2-struktur. XI. Struktur und eigenschaften der verbindungen ACd2×2 (A: Eu, Yb; X: P, As, Sb), Z. Anorg. Allg. Chem. 622 (4) (1996) 679–682, https://doi.org/10.1002/zaac.19966220418.

[11] H.U. Schuster, H.O. Fischer, CeLi2As2, eine ternäre verbindung im CaAl2Si2- Typ/CeLi2As2, a ternary compound in the CaAl2Si2-type, Z. Naturforsch. B 34 (1979) 1169–1170, https://doi.org/10.1515/znb-1979-0828.

[12] H.O. Fischer, H.U. Schuster, Preparation and crystal structure of $PrLi_2P_2$, $PrLi_2As_2$ and $NdLi_2As_2$, Zeitschrift fuer Naturforschung Teil B: Anorganische Chemie, Organische Chemie, Biochemie, Biophysik, Biologie 35 (10) (1980) 1322–1323.

[13] G. Zwiener, H. Neumann, H.-U. Schuster, Magnetische Eigenschaften von AB2X2-Verbindungen im CaAl2Si2-Typ/Magnetic Properties of AB2X2 Compounds with the CaAl2Si2 Structure, Z. Naturforsch. B. 36 (1981) 1195–1197.

[14] I. Grund, H.-U. Schuster, P. MuÈ ller, Ternäre Verbindungen von Lithium mit Yttrium, Lanthan bzw. Neodym und 5b-Elementen im „aufgefüllten" $CaAl_2Si_2$-Typ, Z. Anorg. Allg. Chem. 515 (1984) 151.

[15] V.V. Nemoshkalenko, V.Ya. Nagornyi, B.P. Mamko, P.K. Kikolyuk, P.V. Gel, R.V. Lutsiv, M.D. Koterlin, The electronic structure of triple intermetallic compounds of RAl2 Si2 type, Ukr. Fiz. Zh. 26 (1981) 1831.

[16] V.V. Nemoshkalenko, Electronic Structure of Intermetallic Compounds of the RAl sub 2 Si sub 2 Type, Metallofizika (Akad. Nauk. Ukr. SSR., Otd. Fiz.) 7 (3) (1985) 22.

[17] O.S. Zarechnyuk, A.A. Muravyova, E.I. Gladyshevskii, New intermetallic compounds of La202S-type,Dop, Akad. Nauk. Ukr. RSR Ser. A 32 (1970) 753.

[18] R. Nesper, H.G.v. Schnering, J. Curda, GdAl2Si2, eine unerwartete Verbindung im $CaAl_2Si_2$-Typ [1]/$GdAl_2Si_2$, an Unexpected Compound of the $CaAl_2Si_2$-Type [1], Z. Naturforsch. B 37 (1982) 1514, https://doi.org/10.1021/ja00268a027.

[19] H. Flandorfer, P. Rogl, The crystal structure of two novel compounds: CeAlSi2 and Ce3Al4Si6, J. Solid State Chem. 127 (1996) 308, https://doi.org/10.1006/jssc.1996.0388.

[20] A.A. Muraveva, O.S. Zarechnyuk, E.I. Gladyshevskii, The systems Y–Al–Si (Ge, Sb) in the range 0–33.3 at% Y, Inorg. Mat. 7 (1971) 34.

[21] C. Kranenberg, D. Johrendt, A. Mewis, Untersuchungen zum existenzgebiet des CaAl2Si2-strukturtyps bei ternären siliciden, Z. Anorg. Allg. Chem. 625 (11) (1999) 1787–1793, https://doi.org/10.1002/(SICI)1521-3749(199911)625:11<1787::AID-ZAAC1787>3.0.CO;2-H.

[22] C. Kranenberg, D. Johrendt, A. Mewis, R. Pöttgen, G. Kotzyba, C. Rosenhahn, B.D. Mosel, Structure and properties of the compounds LnAl2×2 (Ln= Eu, Yb; X= Si, Ge), Solid State Sci. 2 (2) (2000) 215–222, https://doi.org/10.1016/S1293-2558(00)00135-7.

[23] K. Rajput, & S. Vitta, Thermoelectric properties of rare earth filled type-I like clathrate, Dy8Al16Si30, J. Mat. Sci. Mat. Elect. *27*, 10303-10308, *arXiv preprint arXiv:1509.08277* (2015). 10.48550/arXiv.1509.08277.

[24] C. Kranenberg, D. Johrendt, A. Mewis, R. Pöttgen, G. Kotzyba, C. Rosenhahn, B.D. Mosel, Structure and properties of the compounds LnAl2×2 (Ln= Eu, Yb; X= Si, Ge), Solid State Sci. 2 (2) (2000) 215–222, https://doi.org/10.1016/S1293-2558(00)00135-7.

[25] C. Kranenberg, D. Johrendt, A. Mewis, The stability range of the CaAl2Si2-type structure in case of LnAl2Ge2 compounds, Solid State Sci. 4 (2) (2002) 261–265, https://doi.org/10.1016/S1293-2558(01)01237-7.

[26] E.J. Gladishevskij, P.I. Kripjakevic, O.I. Bodak, The crystal structures of the compounds CaAl2Si2 and its analogues, Ukr. Fiz. Zh.(Russ. Ed.) 12 (1967) 447–453.

[27] G.Q. Huang, R.D. Miao, Electronic structure and electron–phonon interaction in YAl_2Si_2, Physica B: Condens. Matter 391 (1) (2007) 174–178, https://doi.org/10.1016/j.physb.2006.09.015.

[28] O.S. Zarechnyuk, The Crystal Structure of the Compound YtNi sub 2 Al sub 3 and Related Phases, Vestn. L'vov. Univ.[Khim.] 23 (1981) 45–47.

[29] C. Kranenberg, D. Johrendt, A. Mewis, The stability range of the CaAl2Si2-type structure in case of LnAl2Ge2 compounds, Solid State Sci. 4 (2) (2002) 261–265, https://doi.org/10.1016/S1293-2558(01)01237-7.

[30] P. Klüfers, A. Mewis, AB2X2-Verbindungen im CaAl2Si2-Typ, III Zur Struktur derVerbindungen CaZn2P2, CaCd2P2, CaZn2As2 und CaCd2As2/AB2X2 Compoundswith the CaAl2Si2 Structure, III The Crystal Structure of CaZn2P2, CaCd2P2,CaZn2As2, and CaCd2As2, Z. Naturforsch., B: Chem. Sci. 32 (1977) 753.

[31] P. Hohenberg, W. Kohn, Inhomogeneous electron gas, Phys. Rev. 136 (1964) B864–B871.

[32] W. Kohn, L.J. Sham, Self-consistent equations including exchange and correlation effects, Phys. Rev. 140 (1965) A1133–A1138, https://doi.org/10.1103/PhysRev.140.A1133.

[33] P. Blaha, K. Schwarz, G.K.H. Madsen, D. Kvasnicka, J. Luitz, WIEN2K, An Augmented Plane Wave Plus Local Orbitals Program For Calculating Crystal Properties, Vienna University of Technology, Vienna, 2001.

[34] J.P. Perdew, K. Burke, M. Ernzerhof, Generalized gradient approximation made simple, Phys. Rev. Lett. 77 (1996) 3865, https://doi.org/10.1103/PhysRevLett.77.3865.

[35] A.I. Liechtenstein, V.I. Anisimov, J. Zaanen, Density-functional theory and strong interactions: Orbital ordering in Mott-Hubbard insulators, Phys. Rev. B 52 (1995) R5467, https://doi.org/10.1103/PhysRevB.52.R5467.

[36] O. Bengone, M. Alouani, P. Blochl, J. Hugel, Implementation of the projector augmented-wave LDA+ U method: Application to the electronic structure of NiO, Phys. Rev. B 62 (2000) 16392, https://doi.org/10.1103/PhysRevB.62.16392.

[37] H.J. Monkhorst, J.D. Pack, Special points for Brillouin-zone integrations, Phys. Rev. B 13 (1976) 5188–5192, https://doi.org/10.1103/PhysRevB.13.5188.

[38] J.D. Pack, H.J. Monkhorst, Special points for Brillouin-zone integrations—a reply, Phys. Rev. B 16 (1977) 1748–1749, https://doi.org/10.1103/PhysRevB.16.1748.

[39] Q.D. Gibson, H. Wu, T. Liang, M.N. Ali, N.P. Ong, Q. Huang, R.J. Cava, Magnetic and electronic properties of $CaMn_2Bi_2$: a possible hybridization gap semiconductor, Phys. Rev. B 91 (8) (2015) 085128, https://doi.org/10.1103/PhysRevB.91.085128.

[40] Z. Zada, A.A. Khan, R. Zada, A.H. Reshak, G. Murtaza, M. Saqib, &.J. Bila, First-principles calculations to investigate variation of cationic-ligand LmAl2Ge2 (Lm= Ca, Y, La and Ce), Indian J. Phys. 96 (11) (2022) 3151–3159, https://doi.org/10.1007/s12648-021-02242-7.